

**Conceptual Design of a  
He-cooled Divertor with  
Integrated Flow and Heat  
Transfer Promoters  
(PPCS Subtask TW3-TRP-001-D2)  
Part I: Summary**

**Compiled and edited by**

**R. Kruessmann and P. Norajitra**

**Contributors:**

**L. V. Boccaccini, T. Chehtov, R. Giniyatulin,  
S. Gordeev, T. Ihli, G. Janeschitz,  
A. O. Komarov, W. Krauss, R. Kruessmann,  
V. Kuznetsov, R. Lindau, P. Norajitra, I.  
Ovchinnikov, V. Piotter, M. Rieth,  
R. Ruprecht, V. Slobodtchouk,  
V. A. Smirnov, R. Sunyk**

**Institut für Materialforschung  
Institut für Reaktorsicherheit  
Programm Kernfusion**

**April 2004**

# **Forschungszentrum Karlsruhe**

in der Helmholtz-Gemeinschaft

Wissenschaftliche Berichte

FZKA 6974

## Conceptual Design of a He-cooled Divertor with Integrated Flow and Heat Transfer Promoters (PPCS Subtask TW3-TRP-001-D2)

### **Part I: Summary**

Compiled and edited by R. Kruessmann and P. Norajitra

Contributors:

L. V. Boccaccini, T. Chehtov, R. Giniyatulin<sup>1</sup>, S. Gordeev, T. Ihli,  
G. Janeschitz, A. O. Komarov<sup>1</sup>, W. Krauss, R. Kruessmann,  
V. Kuznetsov<sup>1</sup>, R. Lindau, P. Norajitra, I. Ovchinnikov<sup>1</sup>,  
V. Piotter, M. Rieth, R. Ruprecht, V. Slobodtchouk,  
V. A. Smirnov<sup>1</sup>, R. Sunyk

Institut für Materialforschung  
Institut für Reaktorsicherheit

Programm Kernfusion

<sup>1</sup>D. V. EFREMOV Institute, Scientific Technical Centre „Sintez“,  
St. Petersburg

Forschungszentrum Karlsruhe GmbH, Karlsruhe

2004

**Impressum der Print-Ausgabe:**

**Als Manuskript gedruckt  
Für diesen Bericht behalten wir uns alle Rechte vor**

**Forschungszentrum Karlsruhe GmbH  
Postfach 3640, 76021 Karlsruhe**

**Mitglied der Hermann von Helmholtz-Gemeinschaft  
Deutscher Forschungszentren (HGF)**

**ISSN 0947-8620**

## **Abstract**

Within the framework of the EU power plant conceptual study (PPCS), helium-cooled modular divertor concepts with a flow promoter (HEMP as a pin array and HEMS as slot array version) have been investigated at the Forschungszentrum Karlsruhe since 2002. The design goal is to achieve a high heat flux performance of  $15 \text{ MW/m}^2$ . In this summary of the detailed report, research areas related to the development of a helium-cooled divertor shall be addressed. Latest changes in thermohydraulic layout as well as current results of simulation calculations shall be presented exemplarily for the slot concept HEMS which has the crucial advantage of being easier to manufacture. The divertor construction resulting from the requirements as well as the design-related issues shall be discussed. Possible manufacturing processes for divertor components of tungsten are assessed. Chapters 7 and 8 have been completely revised comprising the latest results of the thermohydraulic layout and thermomechanical analyses. Calculation results have to be verified by experiments. For this purpose, a helium loop will be built at the Efremov Institute, St. Petersburg, Russia, in 2004. An outlook on an alternative multi-jet design (HEMJ) will be given at the end of this report.

## **Konzeptionelles Design eines He-gekühlten Divertors mit integrierter Einheit zur Strömungs- und Wärmetransferverbesserung (PPCS TW3-TRP-001-D2)**

### **Teil 1: Zusammenfassender Bericht**

#### **Zusammenfassung**

Im Rahmen der EU-Reaktorstudie (PPCS) wurden seit 2002 im Forschungszentrum Karlsruhe heliumgekühlte modulare Divertorkonzepte (HEMP als Pin-Array- und HEMS als Slot-Array-Version) untersucht. Ziel ist das Erreichen einer Wärmelastleistung von  $15 \text{ MW/m}^2$ . In diesem zusammenfassenden Bericht zur ausführlichen Version werden die Forschungsgebiete zur Entwicklung eines heliumgekühlten Divertors erörtert. Neueste Änderungen in der thermohydraulischen Auslegung sowie aktuelle Ergebnisse der Simulationsberechnungen werden für das Slot-Konzept HEMS beispielhaft dargestellt, das mit seiner einfacheren Herstellung einen entscheidenden Vorteil hat. Die sich aus den Anforderungen ergebende Divertorkonstruktion sowie die damit verbundenen Themen werden diskutiert. Mögliche Herstellungsverfahren für Divertorbauteile aus Wolfram werden angegeben. Kapitel 7 und 8 wurden komplett überarbeitet und zeigen die aktuellen Ergebnisse der thermohydraulischen und thermomechanischen Simulationsberechnungen. Die Ergebnisse müssen durch Experimente überprüft werden. Zu diesem Zweck soll in diesem Jahr eine Helium-Anlage am Efremov Institut, St. Petersburg, Russland, errichtet werden. Am Ende dieses Berichts wird ein Ausblick auf ein alternatives Multijet-Design (HEMJ) gegeben.

## Table of contents

Abstract .....	I
Zusammenfassung .....	I
Table of contents .....	II
1 Introduction .....	1
2 Design goals and design requirements .....	2
3 Design description of the divertor concept proposed by Forschungszentrum Karlsruhe	3
4 Material issues .....	4
4.1 Tungsten tile .....	4
4.2 Thimble of tungsten alloy .....	4
5 Fabrication technologies .....	5
5.1 Fabrication Methods of the Heat Transfer Promoters from W/W Alloy .....	5
5.2 EDM Processing .....	5
5.3 ECM Processing .....	5
5.4 Laser Sintering/Machining .....	6
5.5 PIM Processing .....	6
5.6 Joining of divertor components .....	6
6 Material data .....	8
7 Thermohydraulic investigations .....	8
7.1 Power balance and overall thermohydraulics layout .....	8
7.2 Computational fluid dynamics (CFD) analyses for slots arrays with FLUENT .....	11
8 Thermomechanic analyses .....	16
8.1 Material data .....	17
8.2 Loading and boundary conditions .....	17
8.3 FE model .....	17
8.4 Results .....	17
9 Helium experiments at EFREMOV .....	19
10 Conclusions and outlook .....	20

## 1 Introduction

Within the framework of the EU power plant conceptual study (PPCS), a helium-cooled modular divertor concept with flow promoter has been investigated since 2002 at the Forschungszentrum Karlsruhe. The design goal of the divertor concepts is to achieve a high heat flux performance of  $15 \text{ MW/m}^2$ , which is proposed for a near-term reactor solution like DEMO. In the current study, the PPCS reactor model C is used as a basis of design and layout. The first conceptual design HEMP proposed is based on the use of pin array as flow promoter, which is described in detail in [0-1]. As an alternative, a slot array flow promoter has been considered, which has the crucial advantage of being easier to manufacture. The following summary report refers to the design option with the slot array (HEMS) as reference version.

The development and optimisation of the divertor concepts require a close link of and iterative approach comprising the main issues of design, analyses, materials, fabrication technology, and experiments, sometimes leading to a compromise under economic aspects (e.g. mass production of some components). Predicting the temperatures and stresses by means of computational fluid dynamics (CFD) and finite element methods (FEM) computer codes is indispensable to ensure that the engineering design limits are not exceeded. In general, the working temperature window of the divertor is limited at the upper limit by the recrystallisation temperature of the refractory alloy used and at the lower limit by its ductile-brittle transition temperature. Enlarging this temperature window is a challenging task of materials development. Up to now, only some data are available for unirradiated refractory metals, and even less for irradiated conditions.

Several fabrication methods for the flow promoter and thimble unit made of tungsten alloy are being investigated at FZK and the Efremov Institute in St. Petersburg, Russia. Promising methods are electric discharge machining (EDM), electrochemical milling (ECM), and powder injection moulding (PIM). Technological studies and experiments are being performed at Efremov with respect to e.g. the joining of the W tile to the thimble of W alloy and of the W thimble to the steel structure by means of high-temperature brazing. A helium loop will be built at Efremov this year for high-heat-flux integral tests of divertor mock-ups and to determine the pressure loss and heat transfer coefficient of the cooling unit for various divertor design variants.

In this summary report of [0-1], all research areas related to the divertor development shall be addressed and presented with the slot array being used as an example. After a description of the design goal which results from a list of requirements that is given in detail in [0-1], the design shall be presented in more detail. Possible manufacturing routes are assessed. In the next part, the results of thermohydraulic and thermomechanical simulations will be shown, which have to be verified by experiments. A short description of an experimental setup under construction will complete this summary report.

For all issues addressed, more detailed information can be found in [0-1]. This especially holds for results that have been obtained simultaneously for design options with different flow promoters. To facilitate referencing to [0-1], all figure, table, and reference numbers have been kept in this summary report. Figures with higher numbers than in [0-1] are shown in this summary report only.

## 2 Design goals and design requirements

General objectives and criteria for the design are: a) resistance to a peak heat load of 10 MW/m<sup>2</sup> at least, b) a modular design instead of large plate structures to reduce thermal stresses, c) the divertor operation temperature window has to be higher than the ductile-brittle transition temperature (DBTT) at the lower boundary and lower than the recrystallisation temperature (RCT) at the upper boundary of the structural components made of refractory alloys under irradiation. The latter requires: d) short heat conduction paths from the plasma-facing side to the cooled surface and transport of the cooling agent as closely as possible to the target plates in order to keep the maximum structure temperature as low as possible, e) high heat transfer coefficients, while the coolant mass flow rate and, therefore, the pressure loss as well as the pumping power are as low as possible, and f) survival a certain number of thermal cycles ( $n \approx 100 - 1000$ ) between operating temperature and room temperature during operation.

### Resulting design specifications for the product

- The divertor is divided into 48 cassettes to facilitate remote handling.
- The poloidal length of the target plate is 1 m, the length of the (almost “cold”) baffles is 0.5 m.
- The outboard target plate is poloidally inclined by 10° relative to the strike plane to reduce the heat load on the surface. For the inboard target plate, this value may be larger.
- The average heat load will be about 5 MW/m<sup>2</sup>, the peak heat load 10 MW/m<sup>2</sup>. The peak will be moving along the target plate in a range of 40 cm. The heat flux profile given by Boccaccini [2-6] will be assumed as working hypothesis for this study.
- An average neutronic heating (volumetric heating) of about 18 W/cm<sup>3</sup> in steel is assumed [2-15].
- The sacrificial layer on the target plates is assumed to be 5 mm thick (minimum 3 mm depending on the heat flux), which should be sufficient for a lifetime of 2 years.
- W has the best sputtering characteristics and thermophysical properties of all sacrificial or armour materials candidates and should therefore be used for the target plate.
- The W tile should be attached separately for reasons of containment integrity against crack growth.
- For the structure directly underneath the target plates, refractory metals are employed. These should have superior thermal characteristics, i.e. a high conductivity, high melting point, and large operation temperature window. At present, WL10 is preferred.
- The basis structure is to consist of ODS steel, provided that a solution can be found for the transition pieces to join the parts made of refractory alloys to the steel parts, since their thermal expansion coefficient is highly different.
- Objectives of the design are a high heat transfer value at low pressure loss. The pumping power due to the pressure loss should not exceed 10% of the thermal energy gain.
- The concept must be feasible for manufacturing in a mass production process. Possible manufacturing technologies are EDM, ECM, laser machining, and PIM (see chapter 5 in [0-1]).

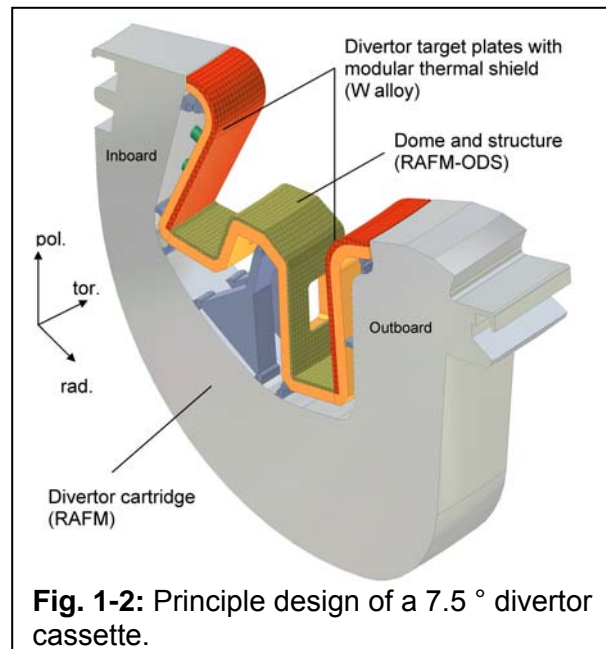
### 3 Design description of the divertor concept proposed by Forschungszentrum Karlsruhe

The divertor is divided into cassettes (Fig. 1-2) for easier handling and maintenance. It is essentially composed of the thermally highly loaded target plates, the dome that contains the opening for removing the particles by vacuum pumps, and the main structure or bulk which houses the manifolds for the coolant.

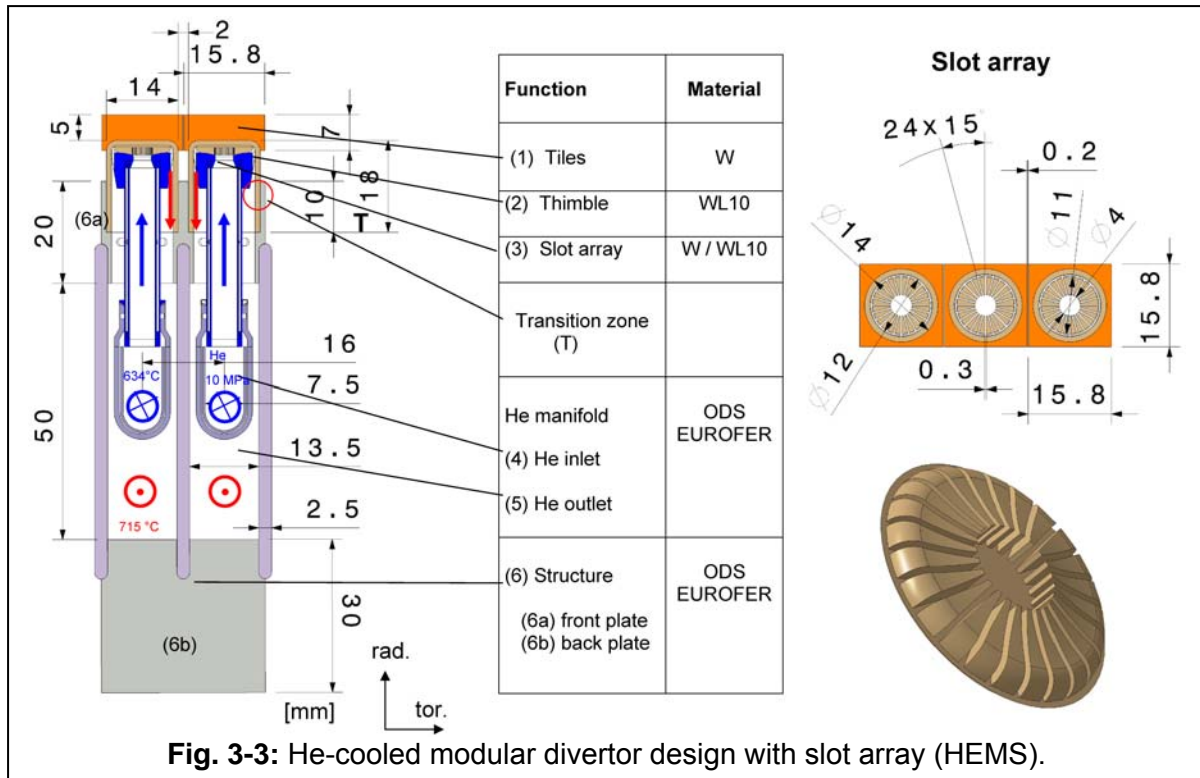
The proposed modular He-cooled divertor concept with integrated slot arrays (HEMS), which is based on the foregoing studies [3-1, 3-2], is illustrated in Fig. 3-3 with a sketch of the cross section of the modules and all dimensions of interest being plotted (left). The numbers in brackets below refer to this figure. Details of the thimble are shown on the right. The concept employs small tiles made of tungsten (1) as thermal shield which is brazed to a finger-like (thimble) structure (2) made of tungsten alloy W-1%La<sub>2</sub>O<sub>3</sub> (WL10). In the first design, these modules have a nominal width of 16 mm. In detail, the W tiles are of quadratic shape with an area of 15.8 x 15.8 mm<sup>2</sup> and 5 mm thick. The thimbles are of cylindrical shape with an outer diameter of 14 mm and a wall thickness of 1 mm. The modules are inserted into a front plate of the structure, which is connected to a back plate by parallel walls. The supporting structures are made of the oxide dispersion-strengthened (ODS) reduced-activation ferritic-martensitic steel EUROFER. A slot array as heat transfer promoter (3) is integrated at the bottom of the thimble by brazing to increase the cooling surface area and, hence, the heat transfer capacity. The slot array is made of tungsten or tungsten alloy.

The divertor is cooled with high-pressure helium at 10 MPa, which is supplied via an inlet manifold (4). Detailed investigation in [0-1] has shown that, generally, it may be chosen between flow through the flow promoter being directed to or off centre. Below, however, flow from the centre outwards shall be preferred and applied as reference case. The He coolant enters the finger unit at a temperature of about 634 °C in the worst case (see below). It is fed upwards through the flow guide tube to the centre of the slot array. After the 90° bend, it flows radially from the centre through the slot array towards the outer edge with high velocity. It is heated up to about 715 °C and routed downwards to the He outlet manifolds (5). Optimisation of the pin or slot arrangement with respect to size, shape, and distance is an important thermohydraulic issue.

The large mismatch in the thermal expansion coefficients of W alloys and the steel structure, which are about  $4\text{-}6 \cdot 10^{-6}/\text{K}$  and  $10\text{-}14 \cdot 10^{-6}/\text{K}$ , respectively, will cause very high local plastic strains at edges and corners in the transition zone (T) under temperature cyclic loadings. To avoid thermocyclic plastification at the joints, an appropriate design of transition pieces is required, which is now under investigation (see [0-1]). A further step in design is the optimisation of the module size in order to minimise the number of modules and, thus, the production costs (current number of modules approx. 300,000).







## 4 Materials issues

### 4.1 Tungsten tile

Tungsten is considered the most promising material that can withstand the specified high heat load, because it possesses a high melting point, high thermal conductivity, and relatively low thermal expansion. In addition, it is low-activating, has a high resistance against sputtering and erosion, and is suitable for use as thermal shield. Its disadvantages are poor DBTT and RCT values, high hardness, and a high brittleness, which make the fabrication of tungsten components comparatively difficult. The tiles have no structural function. A sacrificial layer of 2 mm is foreseen for an estimated service life of about 1-2 years.

### 4.2 Thimble of tungsten alloy

The operation temperature window of the W alloy structures is restricted by the DBTT at the lower and the RCT at the upper boundary. Generally, the DBTT, RCT, and strength properties of W and/or W alloys are determined by the deformation processes and their prehistory as well as by the doping compositions. For irradiated W alloys the presently known temperature window range is extended from 800 to 1200 °C (see also [4-8]).

Tungsten can be alloyed with other refractory elements (e.g. Hf, Ta, Mo, Nb) and noble metals (e.g. Re, Ir, Rh). W-Re alloy, for instance, exhibits excellent DBTT and RCT behaviours in the unirradiated condition and good mechanical properties. Drawbacks in application include its strongly reduced thermal conductivity, its small resources, and its activation. The RCT of W can be improved by adding fine oxide particles (ODS tungsten), such as ThO<sub>2</sub>, La<sub>2</sub>O<sub>3</sub> or Y<sub>2</sub>O<sub>3</sub>. In detail, the W precursors are blended with oxides and subjected to sintering and mechanical processing to achieve high densities. It is assumed that finer grains or ODS particles will positively affect the properties, as it is known from the

use of SPD (severe plastic deformation) techniques e.g. in the fabrication of very thin foils or wires. Further information on the investigations to broaden the operational temperature window can be found in [0-1]. For the current design, W-1%La<sub>2</sub>O<sub>3</sub> will be used for the thimble.

## 5 Fabrication technologies

### 5.1 Fabrication methods of the heat transfer promoters from W/W alloy

Standard tooling methods (e.g. milling) cannot be applied to these materials due to their high hardness and toughness. This particularly holds for parts with a microstructured shape and relatively high aspect ratios (i.e. the ratio between the height and width of the structure).

Requirements are: a) development of a fabrication method for mass production ( $n > 300,000$ ) of divertor components from W or W alloy: heat transfer promoters like pin or slot arrays, thimbles, and tiles, b) development of a fabrication and assembly technology, and testing methods for the divertor-supporting structures of ODS RAFM steel, including manifold and pipe system of the same material.

Feasibility of the required fabrication and application of components from W and/or W alloy has not yet been demonstrated. Therefore, development of fabrication processes is indispensable. Alternative fabrication technologies were studied with respect to their suitability for pin or slot array fabrication. The promising ones shall be pointed out below.

### 5.2 EDM processing

The straight slot concept allows for the application of linear machining technologies, such as sawing or wire EDM.

EDM was favoured for manufacturing the first demonstrators shown in Fig. 5-41, due to the high degree of development of this technology for tool fabrication from hardened steels. The fabrication tests showed that EDM can be applied to generate complicated flow promoter shapes in principle. Two types of electrodes (graphite and copper) can be used to erode tungsten. Processing times and tolerances are similar. The disadvantages of

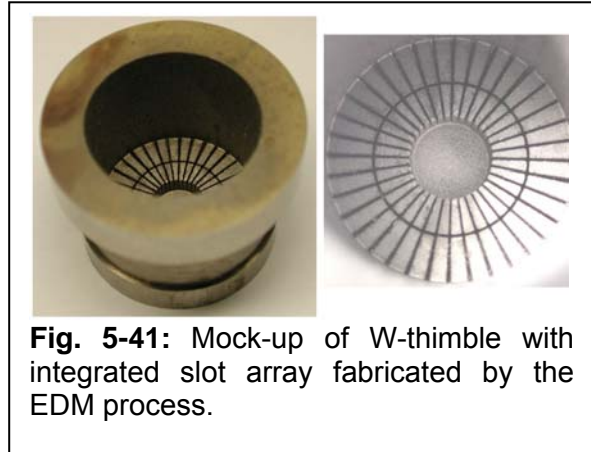


**Fig. 5-41:** Mock-up of W-thimble with integrated slot array fabricated by the EDM process.

the EDM technology are the long processing time of about 30 hours for eroding 2 mm deep arrays and the relatively large wear of the tool, as a result of which frequent replacement is required. It may be used for manufacturing test demonstrators also of flow promoters in the shape of pin and curved slot arrays, but not for mass production.

### 5.3 ECM processing

ECM is a method that has been developed in the last years for the cost-effective fabrication of e.g. steel dies. Its processing time is at least ten times shorter than that of EDM technology. Meanwhile, fine structures have been fabricated in hardened and high-alloyed steels. However, first attempts to structure W with this method failed. This is attributed to surface passivation effects which suppress current flow and stop defined local material removal. Despite this passivation effect observed, ECM remains an attractive solution due to

its short processing times expected. Activities in the field of electrochemistry have been started to solve these passivation problems.

#### 5.4 Laser sintering / machining

Producing the cooling structure in the W thimble by laser machining seems to be very attractive due to its flexibility and accuracy. In this way, it is possible to create most effective patterns with a high cooling efficiency and low pumping power. A first design optimised for the laser technique was made and is now under CFD modelling. First experiments to produce a sample of an Archimedes slot array in W by this method were successful, Fig. 5-42. The surface quality and impact on material properties remain to be checked, this method will be further improved.

It is clear that first investigations show the possibility of cooling pattern production only. The efficiency (and consequently, the costs) of such a process must be improved significantly.

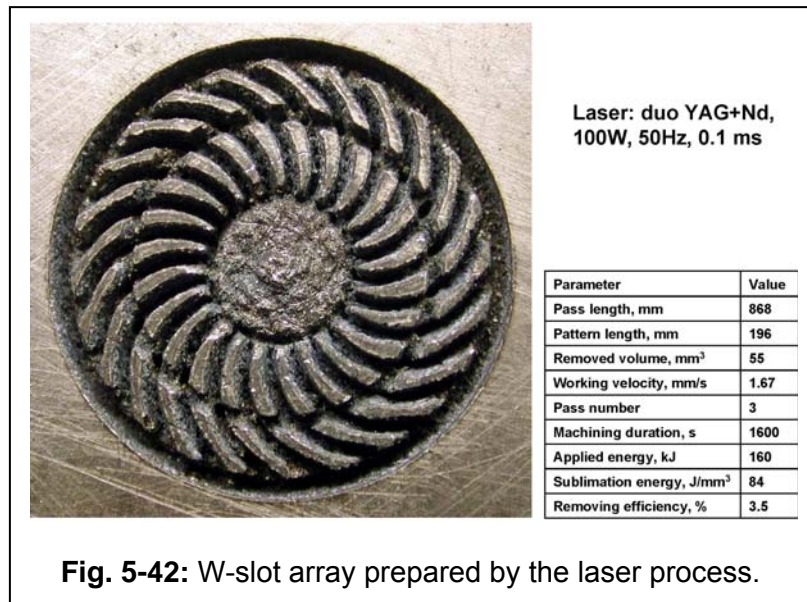


Fig. 5-42: W-slot array prepared by the laser process.

#### 5.5 PIM processing

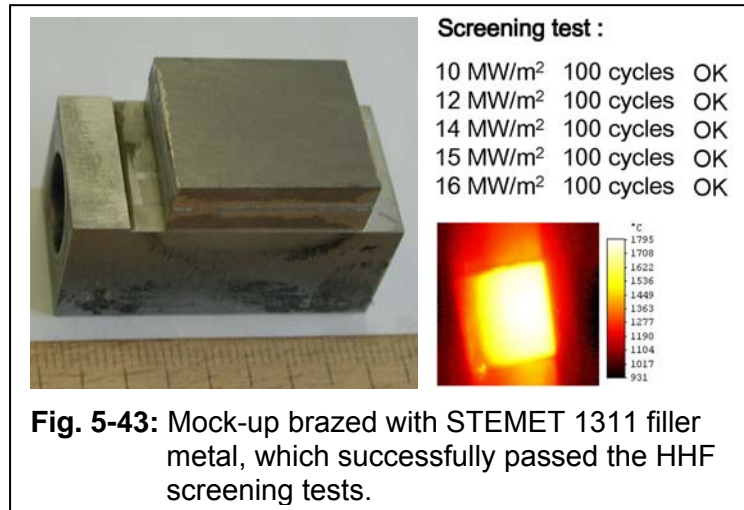
Powder injection moulding (PIM) is one of the well-known fabrication processes in large-scale series production. So far, experience has been gained from the fabrication of micro-structured parts. It is regarded an attractive manufacturing technology for W parts due to its flexibility when working with different designs and different tungsten alloys. Powder consumption for the feedstock can be changed and adapted easily. The PIM process begins with compounding the moulding mass, the so-called feedstock, that consists of about 50vol% polymer binder and powder of the material to be processed. To shape the so-called green compacts, the feedstock is injected into a closed tool with a cavity that consists of feeder and runner systems and moulds having the inverse shape of the green compacts. After this thermoplastic shaping process, the green compacts are released from binders and become the so-called brown compacts which are then sintered to dense products at about 2500 °C for W. First PIM experiments using fine tungsten powder with a particle size of about 1 µm have been started. It remains to be found out whether a sufficiently high thermal conductivity and strength can be achieved.

#### 5.6 Joining of divertor components

In divertor application two types of joints of divertor components, which meet different requirements, are needed. The first type is the joint between the W tile and the thimble of W alloy at high temperature and the second one is needed between the W alloy thimble and steel structure at medium temperature. Welding is not applicable here due to problems of grain growth and other microstructural changes of the W and ODS alloys during joining.

Therefore, high-temperature brazing and diffusion bonding are considered alternative methods.

For the W/W joint between the tile and thimble which are mechanically decoupled from each other, a sufficient ductility of the brazing material is required to successfully stop the crack growth initiated from the top surface of the W tile. The best performance of W/W high-temperature brazing was achieved with the following two filling metal alloys: 71KHCP (Co-based, 5.8 Fe, 12.4 Ni, 6.7 Si, 3.8 B, 0.1 Mn,  $P \leq 0.015$ ,  $S \leq 0.015$ ,  $C \leq 0.08$ ),  $T_{br} = 1100 \text{ }^\circ\text{C}$  and STEMET 1311 (Ni-based, 16.0 Co, 5.0 Fe, 4.0 Si, 4.0 B, 0.4 Cr),  $T_{br} = 1050 \text{ }^\circ\text{C}$ .

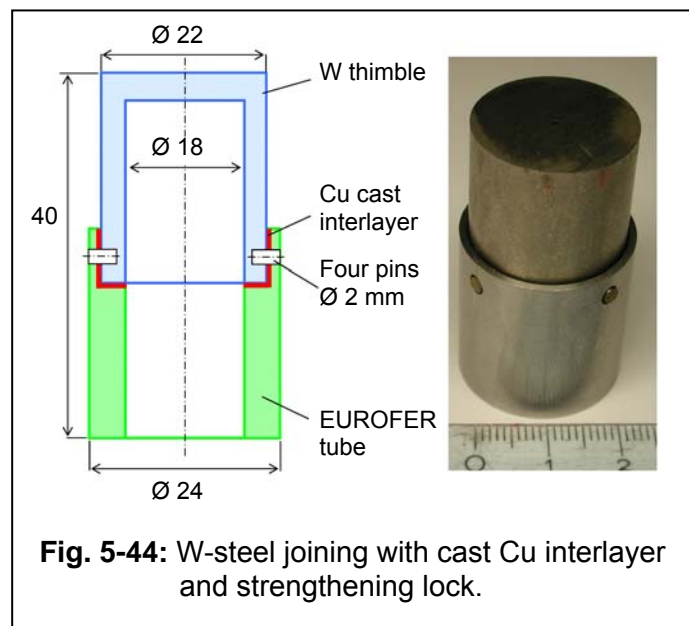


During preliminary tests at Efremov, the mock-ups brazed with 71KHCP survived up to 22 MW/m<sup>2</sup>, those with STEMET 1311 up to 16.5 MW/m<sup>2</sup> (shown in Fig. 5-43). The W/W mock-ups even survived 100 cycles of temperature transient fatigue tests under a heat load of 16 MW/m<sup>2</sup> and a maximum W-W interface temperature of 1200 °C.

However, most of these alloys are no low-activation alloys (e.g. Ni, Ni-Cu, Au-Pd, Zr-Mo, Rh, Ni-Mo-Fe-Cr-Si, or the Ni-, B-, Si-containing STEMET brazing alloys). Since they are used in very small quantities only, they might be tolerable. Their behaviour under irradiation has to be investigated. Brazing temperatures range from 1000 to 2000 °C depending on the alloy composition.

To join the W thimble to the steel structure, the new brazing alloy STEMET 9 could be applied. An Fe-Ni interlayer is necessary to decrease the mismatch of the thermal expansion coefficients of W and FeS. Composition of STEMET 9: Ni-Fe-Mo-Cr-Si-B;  $T_{br}$  about 1200 °C. Other variants of joining the W thimble to the steel structure are being investigated: i) W-steel joining with cast Cu interlayer and strengthening bayonet lock (construction: upper tungsten thimble/supported tube (EUROFER)/filling with cast copper after assembly), mock-up tests are running. ii) W-steel joining with cast Cu interlayer and strengthening lock via four W pins and Cu cast layer (see Fig. 5-44, the mock-up is being tested at the moment).

Apart from the lack of activation, some of these brazing alloys (Ni-, Pd-containing) will probably reduce the recrystallisation temperature of tungsten. The long-term behaviour of none of such joints has been tested at high temperatures so far.



## 6 Materials data

Please refer to [0-1].

## 7 Thermohydraulic investigations

### 7.1 Power balance and overall thermohydraulics layout

T. Ihli, R. Kruessmann, P. Norajitra

#### Requirements

The boundary conditions for the thermohydraulic divertor layout are given by a) the total heat loads and b) the position and shape of the loading curves, which depend on strike point movements (Fig. 7-1).

On the basis of an electric output of the power plant of 1500 MW, the fusion power was determined to be 3410 MW, assuming a net efficiency for the blanket cycle of 0.43 and an energy multiplication factor of 1.17. The total divertor power amounts to 583 MW. It consists of 335 MW neutron-generated heat power for the divertor bulk (256.2 MW) and target plates (44.1 MW OB, 34.7 MW IB, total 78.8 MW) and 248 MW surface heat power (alpha and heating power) for the divertor target. A power distribution between inboard and outboard targets of 1:4 was assumed, thus leading to a surface heat power of 49.6 MW and 198.4 MW for the inboard and outboard target, respectively (Tab. 7-1). For a 7.5° divertor cassette the size of an outboard target plate is about 810 mm x 1000 mm (toroidal x poloidal), leading to an overall average surface heat load of about 3.5 MW/m<sup>2</sup> for all target plates, i.e. 5.1 MW/m<sup>2</sup> for the outboard target plates. These heat loads have to be managed by any divertor design.

**Table 7-1:** Total energy balance of a model C divertor.

	Toroidal sum of 48 cassettes				Values for one cassette	
	Surface heat power $Q_{\alpha} + Q_{\text{heating}}$ (56%OB, 44%IB) (MW) (A)	$Q_{\text{neutron, (56%OB, 44%IB)}}$ (MW)				$Q_{\text{surf.}+\text{neutr.}}$ (MW) (A+B)
		Target plates *)	Bulk	Sum (B)		
<b>Outboard (OB)</b>	<b>198.4</b>	<b>44.1</b>	<b>143.5</b>	<b>187.6</b>	<b>386</b>	<b>8.042</b>
Inboard (IB)	49.6	34.7	112.7	147.4	197	4.104
Sum	248	78.8	256.2	335	583	12.146

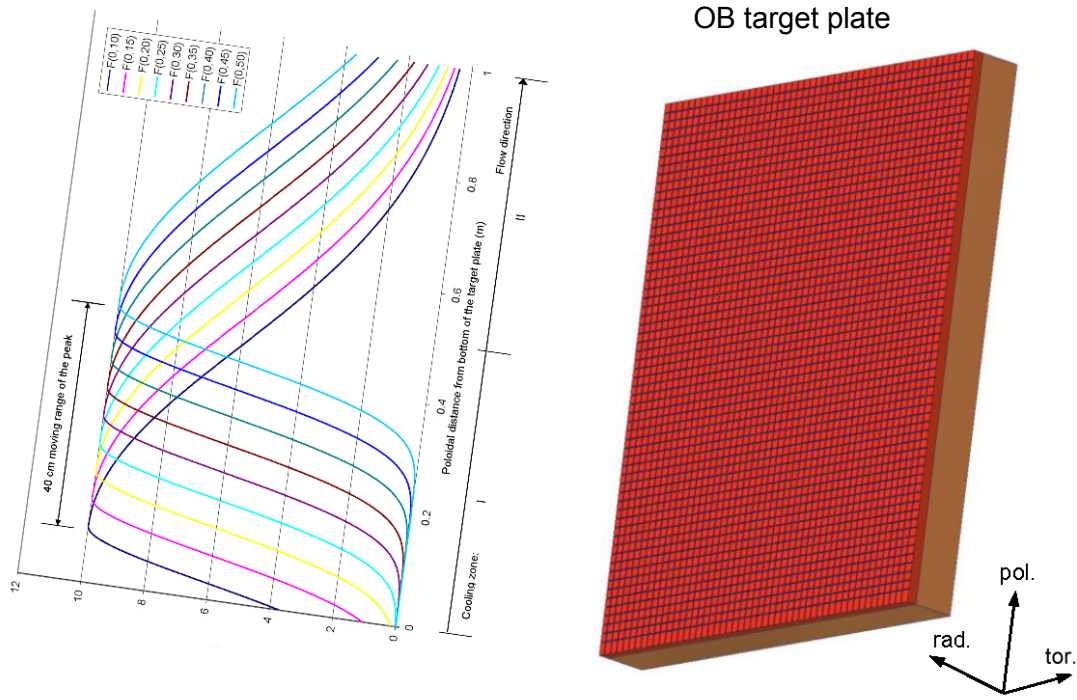


**Fig. 7-1:** Poloidal surface heat load distribution for the outboard target plate.

The high-heat flux (HHF) area of the outboard target plate is determined to have a length of 1 m. Thermal load on the outboard target is defined by the following equations [2-6]:

$$I(z) = I_c + \{ (I_0 - I_c) \cdot \exp[-(z/z_1)^2] \} \quad \text{for } z < 0 \quad (7-1)$$

$$I(z) = I_c + \{ (I_0 - I_c) \cdot \exp[-(z/z_2)^2] \} \quad \text{for } z > 0 \quad (7-2)$$

in a local co-ordinate system in which  $z = 0$  corresponds to the strike point. The values of the parameters that define this curve are:

$$I_0 = 10 \text{ MW/m}^2 \quad I_c = 0 \text{ MW/m}^2 \quad z_1 = 0.07 \text{ m} \quad z_2 = 0.50 \text{ m}$$

The position of the strike point on the 1 m plate is in the interval from 0.1 to 0.5 m referring to the co-ordinate system  $x$  starting from the edge of the plate (dome side). In addition to this load, also the neutronic (volumetric) load is taken into account. This additional heating corresponds to about  $1.13 \text{ MW/m}^2$  (average) for the 1 m target.

### Determination of worst-case and layout parameters

The divertor has to fulfil the requirements (e.g. temperature and stress limits of used materials) over the whole target surface for each strike point position. Therefore, the worst case has to be determined for the thermohydraulic and mechanical layout. The inlet temperature rise in poloidal direction due to coolant heating has to be taken into account, since a higher coolant temperature lowers heat flux. The critical point can be resolved by analyzing the heat transfer coefficient (h.t.c.) that is necessary to fulfil the cooling requirements for each strike point position. The necessary h.t.c. can be calculated as follows:

$$htc_{nec} = \frac{I(z)}{T_{w,mean}(z) - T_{c,mean}(z)} \cdot C_{surf} \quad (7-3)$$

where  $T_{w,mean}$  is the mean wall temperature of the cooling surface in the slot array of one finger,  $T_{c,mean}$  is the mean coolant temperature in a cooling finger, which depends on the strike point position and cooling zone number.  $C_{surf}$  is the surface ratio (target surface / cooling surface). The value of  $C_{surf}$  for the present HEMS geometry is 0.85. At the critical strike point position, a maximum of  $h.t.c_{nec.}$  is detected.

As  $T_{c,mean}$  is a function of layout parameters (mass flow, inlet temperature, number of cooling zones), determination of layout and worst-case parameters is an iterative procedure, leading to the following results: in the present layout, the divertor target plate (length = 1 m) is divided into two zones which are connected in series. All finger units in one zone are connected in parallel. Taking the necessary finger unit mass flow into account, the total mass flow of the divertor would be too high, if all finger units were connected in parallel. For the HEMS concept with slot array (24 straight slots, gaps 0.3 mm) the CFD calculation predicts a sufficient cooling performance for an He inlet pressure of 10 MPa and a He mass flow of about 6 g/s per tile (size 16x16 mm). In each cooling zone (of 0.5 m length each) of the outboard high-heat-flux area (1 m), 31 cooling fingers are arranged in poloidal direction. For these 31 parallel fingers a total mass flow of 188 g/s is necessary to obtain the required cooling performance. For one outboard divertor plate 51 parallel rows are arranged in toroidal direction. This results in a total mass flow of one divertor outboard plate of about 9.6 kg/s.

In Fig. 7-2 the critical strike point position and the heat load curve are shown as well as the corresponding He temperatures at the finger inlet (corresponds to the temperature in the coolant supply channel), finger outlet, and in the coolant return channel. As the He inlet temperature in zone II is higher than in zone I, the worst case occurs, when the strike point position is worse for the first finger units of zone II.

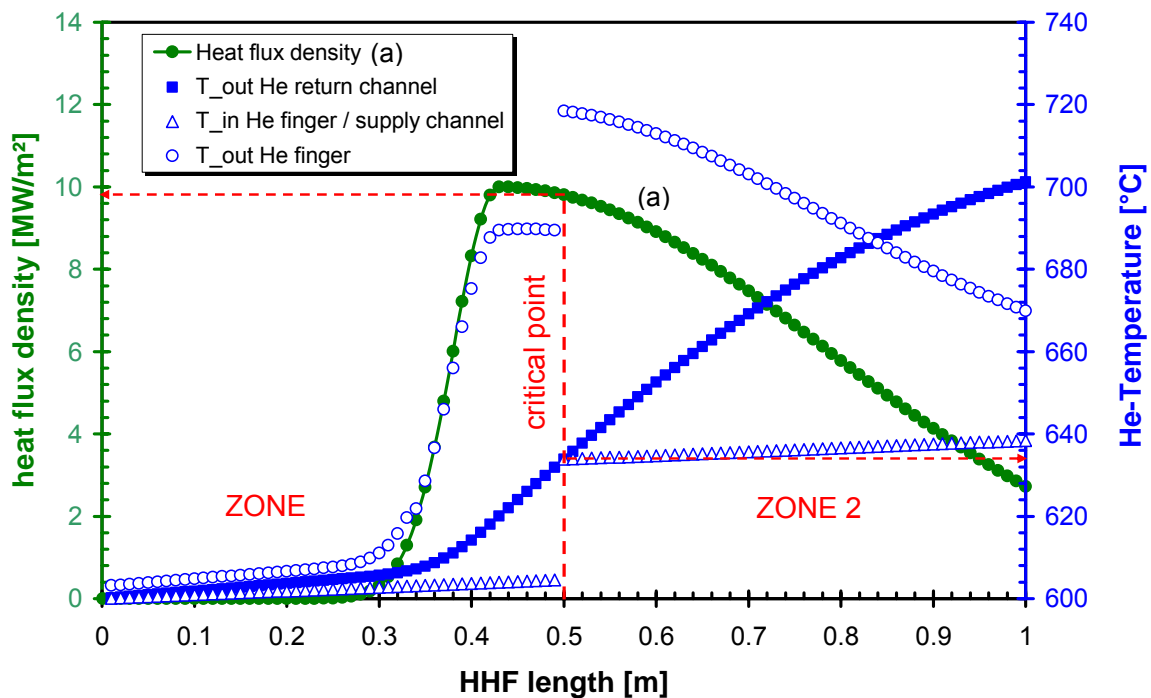


**Fig. 7-2:** He inlet temperature, outlet temperature, and heat flux density vs. target length for the critical strike point position.

The layout and worst-case finger parameters are given in Tab. 7-2. The mean temperature of the slot surface at the critical point (about 10 MW/m<sup>2</sup>) amounts to about 975 °C.

**Table 7-2:** Main layout parameters of one OB divertor plate.

<p><b>He inlet and outlet temperatures:</b></p> <ul style="list-style-type: none"> <li>- Cassette: <math>T_{in} = 540 \text{ °C}</math>, <math>T_{out} = 717 \text{ °C}</math>, <math>\Delta T = 177 \text{ K}</math></li> <li>- OB target plate: <math>T_{in} = 600 \text{ °C}</math>, <math>T_{out} = 701 \text{ °C}</math>, <math>\Delta T = 101 \text{ K}</math></li> <li>- Critical finger unit: <math>T_{in} = 634 \text{ °C}</math>, <math>T_{out} = 718 \text{ °C}</math>, <math>\Delta T = 84 \text{ K}</math>, <math>I = 9.81 \text{ MW/m}^2</math></li> </ul>
<p><b>He mass flow rates:</b></p> <ul style="list-style-type: none"> <li>- One outboard target plate: 9.6 kg/s</li> <li>- One poloidal row of fingers: <math>9.6 / 51 = 0.188 \text{ kg/s}</math></li> <li>- One finger = <math>0.188 / 31 \text{ kg/s} = 0.006 \text{ kg/s}</math></li> </ul>

For the layout parameters described above, the pressure loss of the divertor can be calculated. The pressure loss value of the outboard divertor plate was determined to be about 0.35 MPa and the total pressure loss of the divertor cassette about 0.44 MPa (Tab. 7-3). For the inboard plate an additional mass flow of 3.946 kg/s was determined. Therefore, the total mass flow of one divertor cassette is 13.546 kg/s and of the whole divertor 650.21 kg. From this, the total divertor isentropic compressor power can be calculated to be about 50 MW. In relation to the divertor output heat power of 583 MW, this means a relative pressure loss of 8.6%.

**Table 7-3:** Pressure drop and compressor power calculated for the HEMS layout.

Pressure Loss									
SLOT	Add. Module Unit	Module Unit	HHF Serial connection	Sum HHF Modules	Add. LHF Modules	Sum Modules	Support for Module Units	Bulk	Sum Cassette
MPa	MPa	MPa	-	MPa	MPa	MPa	MPa	MPa	MPa
0.1062	0.0663	0.1726	2	0.3452	0.0500	0.3952	0.0262	0.0221	<b>0.4434</b>
Compressor Power									
Heat Power	He Temp	Mass flow divertor	kappa	R	del_p	p_in	Compressor Power	Compressor Power vs. Heat Power	
MW	°C	kg/s	-	J/(kgK)	MPa	MPa	MW	%	
583	540	650.21	1.67	2078.75	0.44	10.00	50.3	<b>8.6</b>	

## 7.2 Computational fluid dynamics (CFD) analyses for slots arrays with FLUENT

R. Kruessmann

This part presents the results of the CFD calculations that have been obtained for one sample geometry only under the boundary conditions established above for the reference case: slots, 24 straight, parallel channels, width 0.3 mm with flow from the centre to the outside. The mass flow is 6.03 g/s with an inlet temperature of 634 °C. The materials properties will be considered for a mean temperature between the inlet and the outlet temperature of the divertor. Correlations to calculate the properties of helium can be found in chapter 6. Tile, thimble, and insert for enhanced heat transfer were assumed to be made of tungsten. Materials data were chosen according to the ITER Material Properties Handbook



[6-2]. Volumetric heating was not included in the CFD calculations. For all other geometries and boundary conditions, results can be found in [0-1].

As for the preliminary study, about 100,000 hexagonal cells were used to simulate 1/4 of the module in FLUENT. The standard k-ε model was used as well. Other turbulence models have not yet been tested. The value for the density was fixed to be 4.7 kg/m<sup>3</sup>. For the surface roughness, the default values of the program were used.

Results can be found in Tab. 7-7 and in Figs. 7-21 to 7-24. Differences from the results presented in Tab. 7-2 are mainly due to the fact that the additional neutron heating was not included in the FLUENT calculations. Fig. 7-21 shows the temperatures in the tile and thimble in a diagonal cut. With a maximum of 1297 °C for the tile, they fulfil the design limitations. Fig. 7-22 shows the velocity distribution within the slots. Flow is accelerated along the slots. Flow rate in the lower part is smaller. Fig. 7-23 shows the total pressure loss, Fig. 7-24 the static pressure distribution. The highest losses are caused by the flow diversion at the inlet and outlet of the slots and jet impingement cooling at the outlet. An improved design of this area is highly recommended. The overall pressure drop was calculated to be 0.11 MPa which is the surface-averaged total pressure difference between the inlet and outlet surface. The maximum velocity is 202 m/s. The total energy balance was fulfilled with an accuracy of 3%.

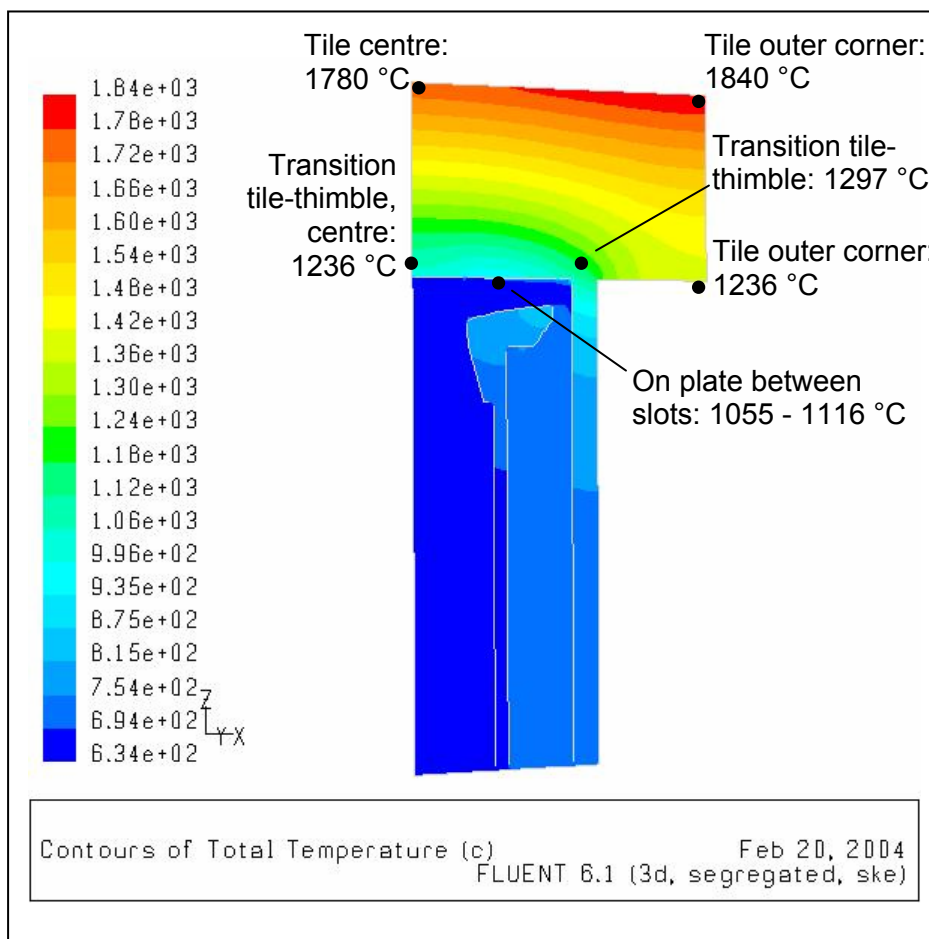


**Fig. 7-21:** Temperature distribution in the diagonal cut through half of the HEMS cooling finger.

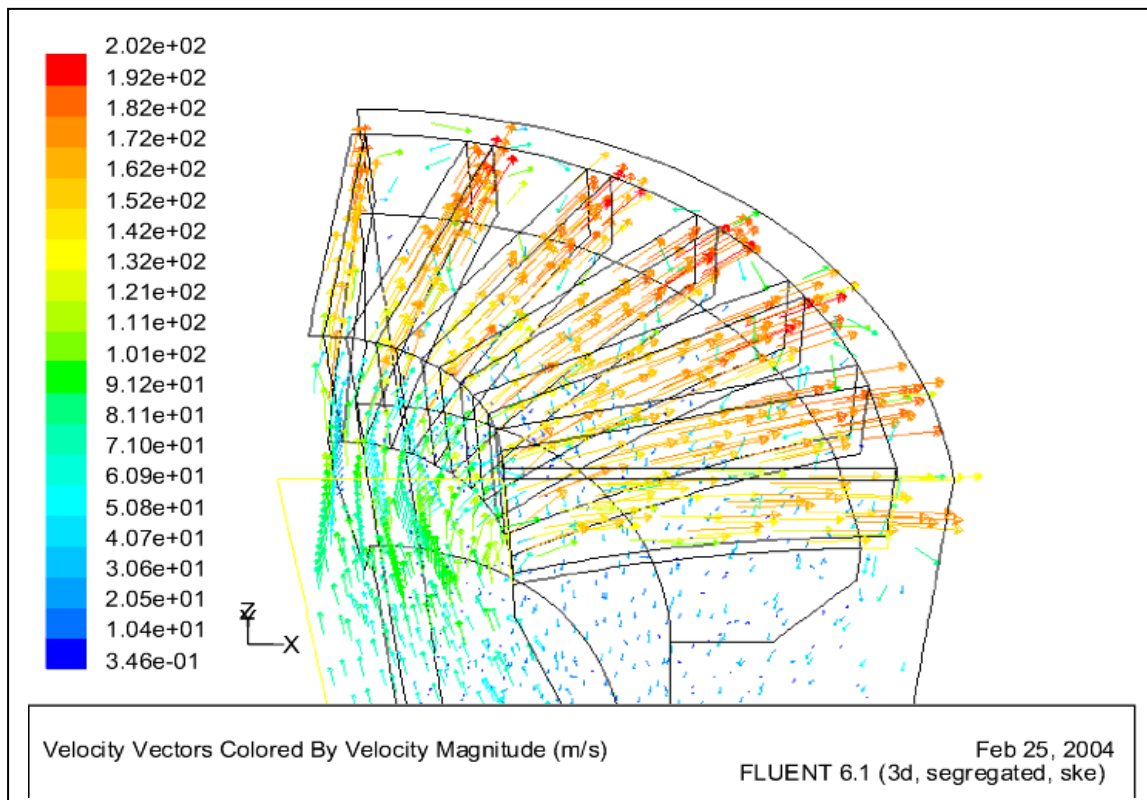


**Fig. 7-22:** Velocity distribution in the slots of the HEMS design.

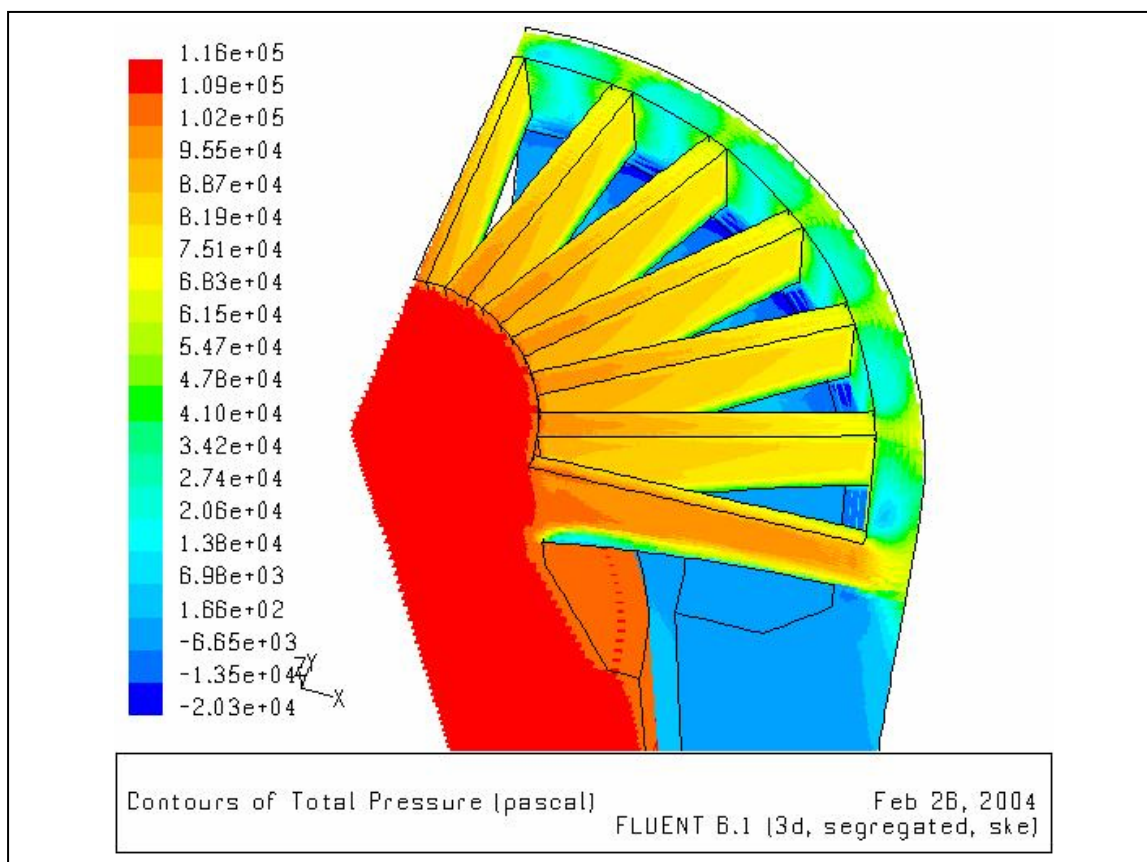


**Fig. 7-23:** Total pressure distribution in the slots of the HEMS design.

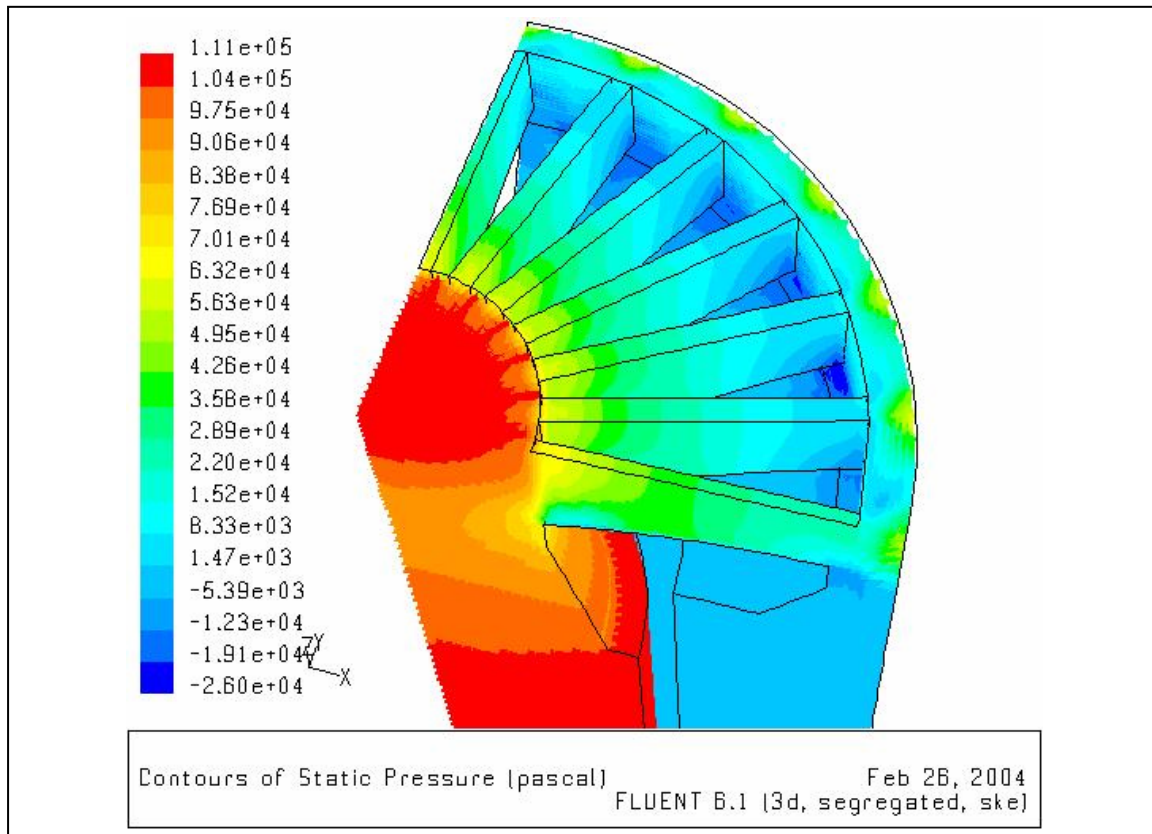


**Fig. 7-24:** Static pressure distribution in the slots of the HEMS design.

The heat transfer coefficient is calculated on the basis of the wall and fluid temperatures and defined locally. It is highest on the lateral sides of the slots near the bottom of the fin plate at the inlet face of the slots and lowest at the bottom of the slots (see Fig. 7-25). Its mean value on the lateral sides of the slots amounts to 24632 W/m<sup>2</sup>K, with local peaks up to 43300 W/m<sup>2</sup>K.

**Table 7-7:** Results of CFD calculations with FLUENT under the boundary conditions of the reference design.

He coolant: <ul style="list-style-type: none"> <li>– Inlet temperature: 634 °C</li> <li>– Outlet temperature 713 °C</li> <li>– Pressure loss <math>\Delta p</math> total 0.11 MPa</li> <li>– Max. velocity in slots: 202 m/s</li> <li>– h.t.c.: local max. 43300 W/m<sup>2</sup>K, mean 24631.73</li> </ul>
Maximum temperature  Tungsten tile: 1840 °C Tungsten structure (thimble): 1297 °C

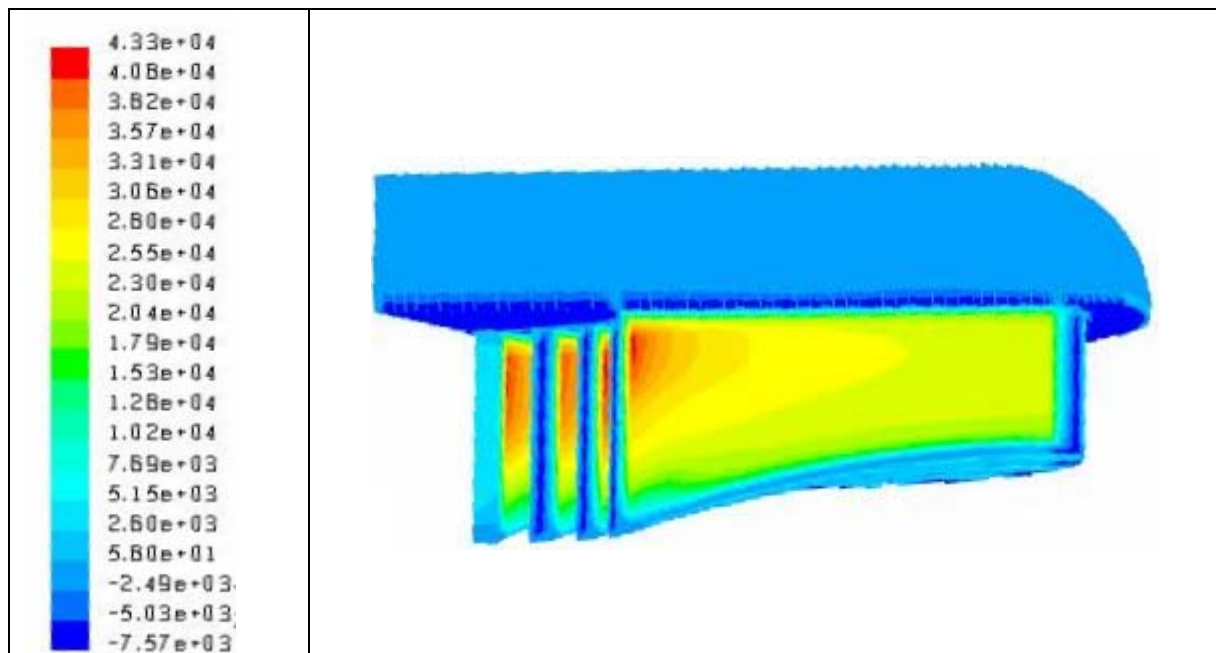


**Fig. 7-25:** Local heat transfer coefficient ( $W/m^2K$ ) on the slot side walls.

In a tentative parameter study that includes also other geometries, it was found that in general straight slots have almost 50% less pressure loss than arrays of circular pins. 24 slots are better than 12, because the temperatures of the tile and thimble are lower. Spread slots (with non-parallel walls) do not result in considerable advantages over straight slots. The choice between these options might depend on manufacturing issues.

For the modular design options considered, it is better to lead the coolant flow from the centre to the outside than vice versa. This results in better cooling of the outer edge of the tile. In this way, the maximum temperatures in the tile and the thimble can be kept smaller due to a better uniformity of the temperature distribution achieved.

The study of flow path lines reveals critical zones for the optimisation of the design. The shape of the entrance into the fin array has to be modified to provide for a better cooling of the outer edges of the tile and to produce a jet effect of the helium. A first attempt was undertaken by introducing an improved nozzle geometry.

### **Summary of the results of the CFD study and outlook**

The intention of the preliminary study was to compare different calculation tools (Fluent, Star-CD, and Ansys Flotran) for use in design analyses during the development of a helium-cooled divertor concept. The results are in reasonable agreement with each other, but differ in some details. They also showed that improvements of the cooling system are necessary. Experiments will be indispensable to validate the simulations. A helium loop for testing different mock-ups is planned by the partners, Forschungszentrum Karlsruhe and EFREMOV Institute in St. Petersburg, including the use of an electron beam facility to provide the necessary high heat fluxes. First experimental results for pressure loss and heat transfer with a different kind of mock-up heating will be obtained at the beginning of 2004, with e-beam heating by 2005.

Preliminary pressure loss experiments carried out at the EFREMOV Institute with a transient set-up showed values which are smaller than the simulated values (at 6 g/s about 0.85 MPa

for the experiments which include manifolds, 0.09 MPa for the simulations of one finger). The discrepancy has to be solved by an improved set-up.

Nevertheless, the preliminary study together with the new overall thermohydraulic concept leads to a reference design with a slot array of 24 slots and a helium mass flow of 6.03 g/s. Based on this design, the CFD calculations will be continued systematically with a parameter study. Parameters are e.g. mass flow, inlet temperature and pressure, temperature rise, etc., but also design variants like curved slots. Effects introduced by the small dimensions (microchannels) will be considered, too. By the end of 2004, the most appropriate design option from the thermohydraulic point of view will be chosen. The influence of different turbulence models as well as of relative surface roughness on the simulation results remains to be investigated.

## 8 Thermomechanical analyses

T. Ihli

This chapter presents results of a thermomechanical simulation of a finger unit (tile/thimble) and consists of two contributions: the temperature distribution obtained by solving a thermal conductivity problem and the stress distribution due to a high-temperature gradient as well as pressure of the coolant (He). These simulations were completely revised after changing the overall thermohydraulic layout and, therefore, they are not included in [0-1].

Both analyses are performed with the FE code ANSYS 8 [7-9]. The 3D model of a finger unit used for both simulations is shown in Fig. 8-30. The model includes a tile and thimble.

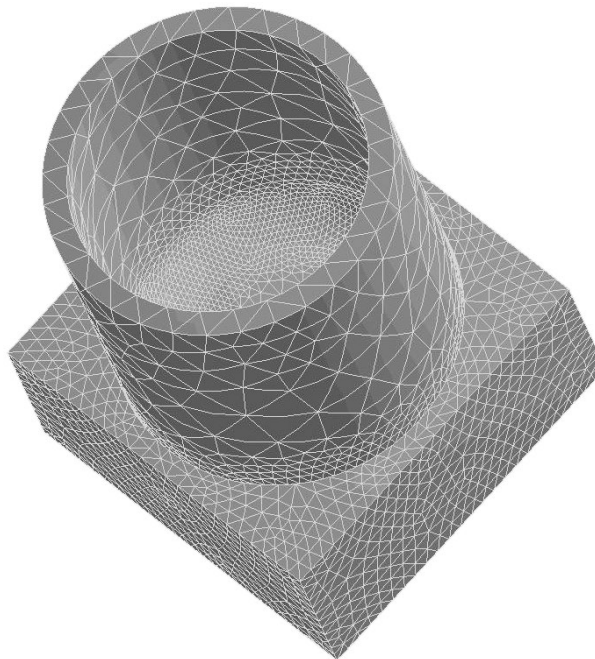


**Fig. 8-30:** Mesh of 3D model.

### 8.1 Materials data

All materials data used have been taken from the Appendix-B of the EFDA requirements document.

### 8.2 Loading and boundary conditions

A thermohydraulic simulation of the finger unit has been performed by R. Kruessmann. Main parameters for the thimble layout are the maximum temperature that was calculated to be about 1297°C and the temperature gradient in the thimble.

Loads and boundary conditions used in this study were surface heat load on the tile (10 MW/m<sup>2</sup>) and an internal pressure load in the thimble (10 MPa). As in previous studies [0-1], high stress levels were detected in the inner corner region of the thimble, the corner radius was therefore increased from 1 to 2 mm to reduce these stress peaks. To obtain the temperature field in the tile and thimble, the heat transfer coefficient inside the thimble was set using the calculated slot heat transfer coefficients and the surface ratio. Comparison of the thimble temperature fields calculated by the FE code and the CFD code (Fluent) showed a high conformity. As the slot is brazed inside the thimble, mechanical connection is weak and the stiffening due to the slot array can be neglected in the stress calculation as long as the temperature field in the thimble resembles the CFD results.

### 8.3 FE model

Fig. 8-30 depicts the meshed model which consists of 107198 nodes and 70102 elements.

### 8.4 Results

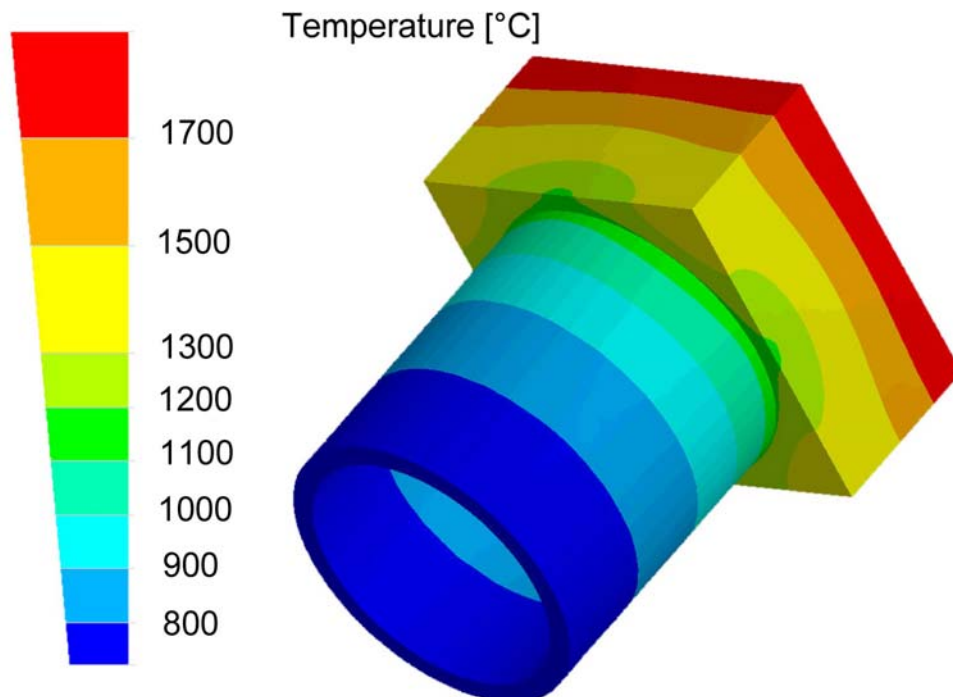


**Fig. 8-31:** Temperature distribution of the tile-thimble assembly.

As described above, the temperature distribution from the CFD calculations was used as setting parameter for the FE calculation. The temperature field of the tile-thimble assembly is shown in Fig. 8-31. The highest temperature in the thimble is about 1300 °C and in the tile up to 1840 °C.

The calculated stress distributions in the tile-thimble assembly are predominantly influenced by the numerical tile-thimble interface treatment. If the tile-thimble interface is assumed to be strongly coupled (“bonded” contact option in the ANSYS workbench tool), the typical stress peak at the curved-flat transition of the thimble bottom disappears when the thimble is analysed separately. The typical stress peak of the separated thimble will be shown in the following calculation (see Fig. 8-33). On the other hand, highest stress levels at the “bonded” tile-thimble assembly occur inside the thimble at the position where the tile ends. If the “no separation” option is set for the tile-thimble interface, a stiffness factor is used to describe the brazing zone behaviour. For the following results this option was assumed to be appropriate to characterise the real interface behaviour.

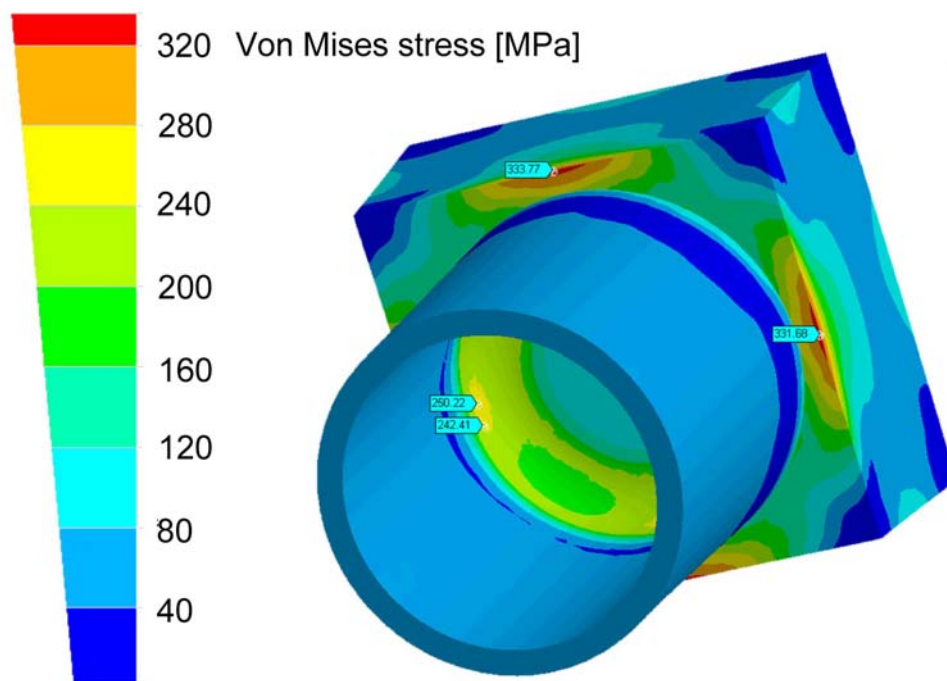


**Fig. 8-32:** Von Mises primary plus secondary stress for the tile-thimble assembly.

The von Mises primary plus secondary stress distribution in the model of thimble and tile is shown in Fig. 8-32. The highest von Mises stress in the thimble is about 250 MPa at a temperature of about 1150 °C. According to the ASME code 3Sm rule, stress levels up to 420 MPa are permissible, and the calculated stress levels in the thimble are far below this limit. The highest stress level of about 335 MPa in the tile occurs at the middle position of the bottom edge of the tile (see Fig. 8-32). As the corresponding temperature is about 1200 °C, the 3Sm rule allows values up to 388 MPa. The stress levels resulting in the whole geometry are acceptable.

As the thimble is a pressure-carrying component, it has to be regarded a safety-relevant part, which should withstand the load even if the tile structure becomes very weak (e.g. due to cracks). Therefore, an additional stress simulation for the separated thimble was carried out (Fig. 8-33). The maximum von Mises stress of the separate thimble is about 300 MPa at a temperature of 1150 °C. Consequently (3Sm = 420 MPa), the requirement of a safe pressure containment with weak tile structure is fulfilled.

Rounding of the thimble with an inner corner radius increased from 1 to 2 mm was sufficient to significantly reduce the stress levels inside the thimble below the permissible values given by the 3Sm rule. It was thus verified that peak stress values (seen in forging studies) can be reduced by relatively small changes in geometry.

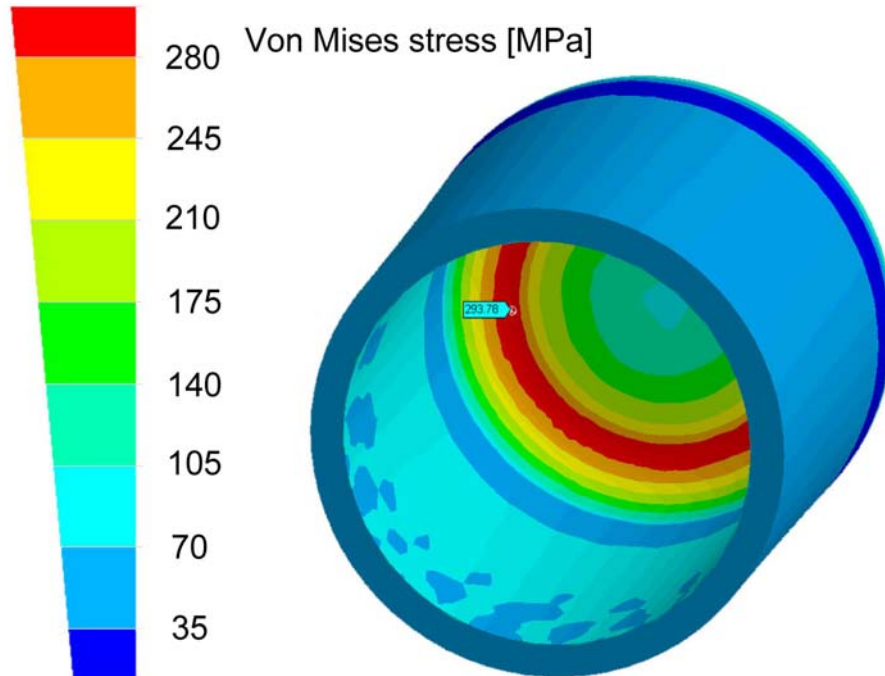


**Fig. 8-33:** Von Mises primary plus secondary stress of the separate thimble.

## 9 Helium experiments at EFREMOV

Pressure loss measurements and h.t.c. determination at the Gas Puffing Facility (GPF) based on a dynamic method

The GPF experiments are based on a reversed heat flux method, i.e. hot helium gas is pumped through the divertor mock-ups to estimate their thermohydraulic efficiency (pressure loss and h.t.c.). In detail, the helium gas is expanded by means of a valve system from a high pressure tank (15 MPa) on one side, heated up, and passed through the mock-up to the second tank with lower pressure (4 MPa) within a short time. The mock-up itself is cooled by water. Temperatures and pressures at the inlet and outlet of the mock-up are measured transiently. To evaluate the HTC results, the mass flow rate and energy balance are determined.

Fig. 9-14 shows the pressure losses of a pin array mock-up measured in GPF1 experiments. The dotted curve (black rhombus) refers to the values extrapolated to the condition of 10 MPa and 700 °C. According to this curve, the pressure loss e.g. at a mass flow rate of 5.5 g/s is about 0.08 MPa, which is smaller than the value predicted by CFD calculations by about a factor of 2. This tendency of pressure loss overestimation by CFD codes generally is observed in any case. The reason for this discrepancy remains to be found out.



# FZK mock-up: hydraulic resistivity

Memo: input pressure vary within 7.5-10 Mpa !

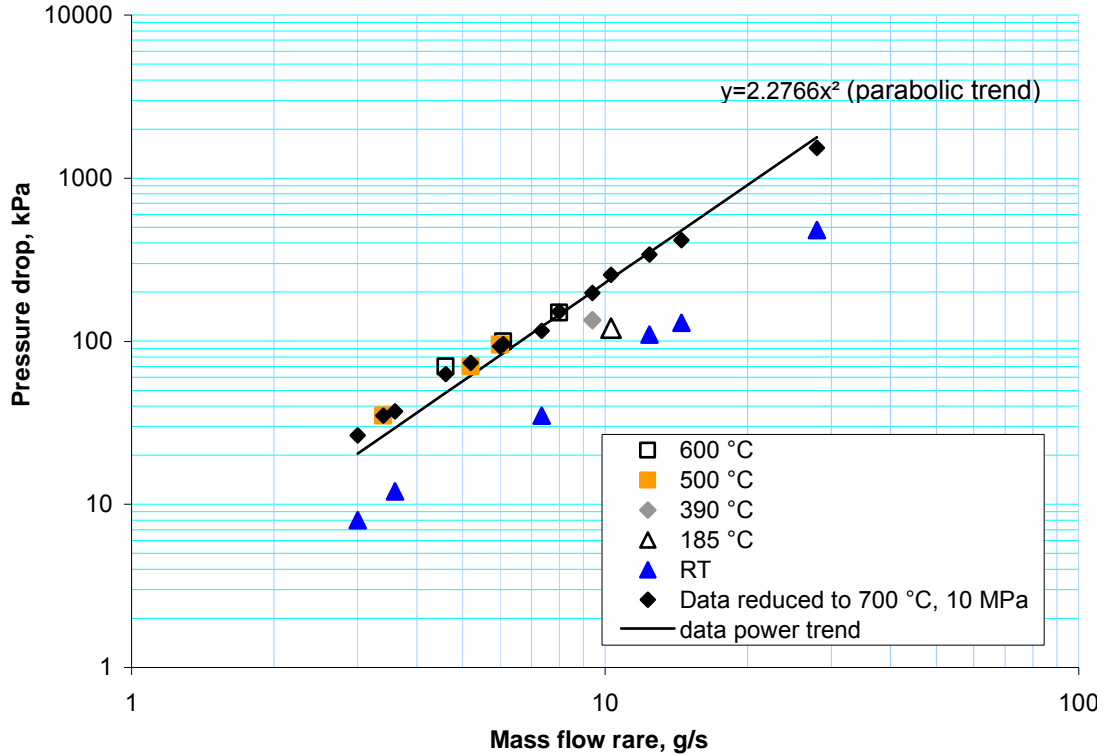


Fig. 9-14: Results of experiments at higher temperatures, data reduced to 700 °C, 10 MPa.

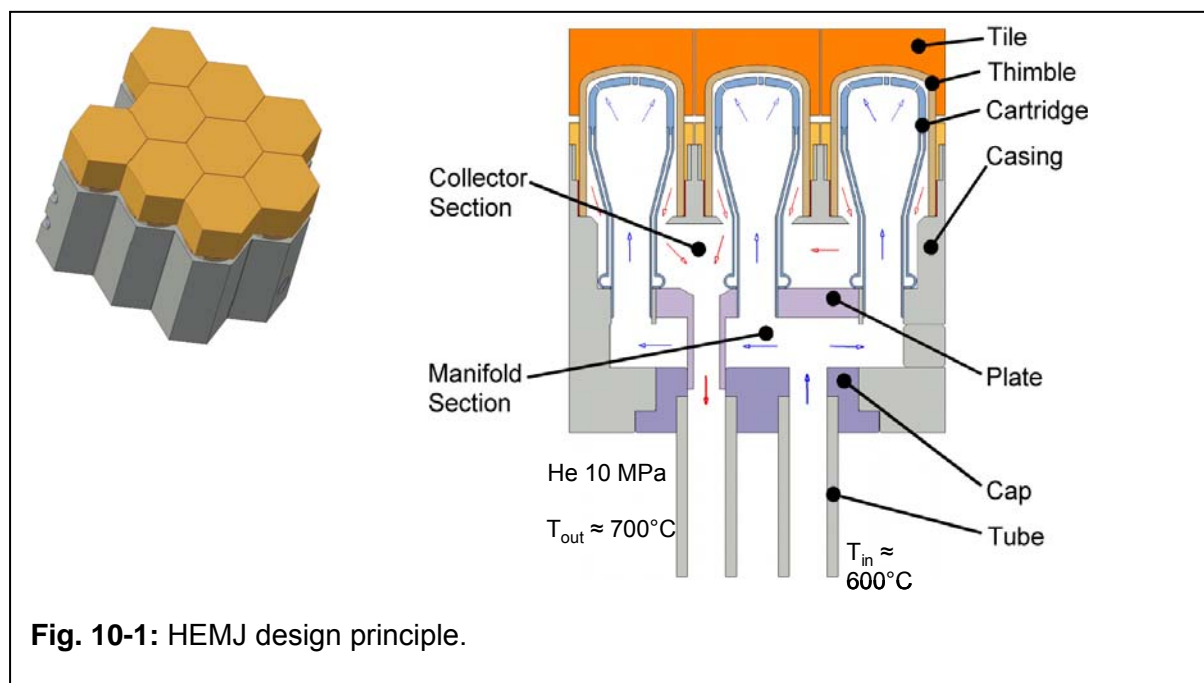
## 10 Conclusions and outlook

A study of helium-cooled divertor concepts with a flow promoter was performed in the major fields of design, analyses, materials, fabrication technology, and experiments. The design goal was to reach a peak heat load of 10 MW/m<sup>2</sup>. Two conceptual designs with different kinds of flow promoter, i.e. pin array (HEMP) and slot array (HEMS), were investigated. The latter has the advantage of being easier to manufacture and is regarded as reference version in this summary report. For manufacturing divertor components of tungsten and tungsten-alloy, EDM, ECM, laser, and PIM are considered promising methods which require further R&D. Technological experiments with respect to W/W and W/steel joints were performed successfully at Efremov, further R&D is needed for improvement. Taking into account the temperature constraints for the tungsten structure and a region of moving peak heat flux, a careful thermohydraulic layout was made, leading to a necessary He mass flow rate of 6 g/s for one divertor finger module. Under the boundary condition of 10 MPa He pressure and 634 °C He inlet temperature at the target, the maximum W structure temperature amounts to 1297 °C (FLUENT) and is below the design limit of 1300 °C given by the recrystallisation temperature of W. The pressure loss was calculated to be 0.35 MPa for the target plate and 0.44 MPa for the whole cassette, corresponding to a pumping power of about 9% related to the heat power to be removed. The stress calculations with ANSYS also show that all

stresses are below the engineering 3Sm limit (maximum primary plus secondary von Mises stress in the thimble amounts to 250 MPa < 420 MPa permissible at 1150 °C).

The overall results of this study show that the He-cooled modular divertor concept (HEMS) meets a large variety of requirements, e.g. loading conditions and materials and fabrication issues, and is viable.

Nevertheless, the divertor design is being improved continuously to simplify the design, reduce the fabrication effort, and increase cooling performance. One of such conceivable concepts is the He-cooled multi-jet (HEMJ) design [10-1], Fig. 10-1, which is based on the multiple jet impingement cooling technology being state-of-the-art for internal cooling in high-temperature machines like gas and steam turbines. This concept possesses many advantages, e.g. jet-to-wall direct cooling without flow promoter, uniform He temperature over the cooling surface, stable mass flow distribution, stable form of the curved thimble bottom, high heat packing density due to hexagonal tile shape, easy exchange and tests of the box units, etc. It is being investigated in detail. First assessments show a promising high potential of limiting the heat flux in the range of 15 MW/m<sup>2</sup>.



Regarding the divertor material, development of W alloys will be needed in the long term to broaden the operational temperature window from the today's range of 800 – 1200°C to 600 – 1300 °C by increasing the recrystallisation temperature and simultaneously lowering the DBTT. Potential use of graded materials shall be considered. Additionally, development of the manufacturing technologies EDM, ECM, laser, and PIM for divertor components made of tungsten or tungsten alloys will be continued.

In addition, a large helium loop is planned to be constructed at the EFREMOV Institute in St. Petersburg, Russia. An electronic beam facility is available there, which allows for the HHF simulation of 10 MW/m<sup>2</sup> at least. Planning and specification of the experiment programs are under way. The loop is scheduled to be in operation by the end of 2004 and to deliver first test results in 2005.

## **Acknowledgement**

This work has been performed within the framework of the Nuclear Fusion Programme of Forschungszentrum Karlsruhe and is supported by the European Union within the European Fusion Technology Programme. The contents of the publication lie in the sole responsibility of the publishers and do not necessarily represent the views of the Commission or its services.

## References

- [0-1] R. Krüssmann, P. Norajitra, L. V. Boccaccini, T. Chehtov, R. Giniyatulin, S. Gordeev, T. Ihli, G. Janeschitz, A. O. Komarov, W. Krauss, V. Kuznetsov, R. Lindau, I. Ovchinnikov, V. Piotter, M. Rieth, R. Ruprecht, Conceptual design of a He-cooled divertor with integrated flow and heat transfer promoters (PPCS Subtask TW3-TRP-001-D2), Part II: Detailed Version. FZKA 6975, 2004.
- [2-6] L.V. Boccaccini, He-Cooled Divertor General Design Requirements Document, Draft Version 1, September 2003 and appendices of February 2004 (unpublished).
- [2-15] U. Fischer, Personal communication, FZK, Oct. 2002.
- [3-1] S. Hermsmeyer and S. Malang, "Gas-cooled high-performance divertor for a power plant", Fusion Engineering and Design, vol. 61-62, pp. 197-202, November 2002.
- [3-2] E. Diegele, R. Krüssmann, S. Malang, P. Norajitra, G. Rizzi, Modular He-cooled divertor for power plant application, Symposium on Fusion Technology, Helsinki, Finland, 9<sup>th</sup> – 13<sup>th</sup> Sept. 2002, Fusion Engineering and Design, 66 – 68 (2003), 383 – 387.
- [4-8] S. Sharafat, R. Martinez, N. M. Ghoniem, APEX Study Group Meeting, PPPL, May 12-14, 1999.
- [6-2] ITER Material Properties Handbook, 2001.
- [7-9] ANSYS 8 (ANSYS, Inc.), 2003.
- [10-1] T. Ihli, P. Norajitra, G. Janeschitz, R. Krüssmann, R. Ruprecht, Development of an advanced Helium-jet-cooled divertor concept: cooling method and design, Jahrestagung der Kerntechnischen Gesellschaft Deutschland, Düsseldorf, 25<sup>th</sup> – 27<sup>th</sup> May 2004, to be published.